

Biological oxidations and nitrations promoted by hemin- $A\beta_{16}$ complex

Silvia De Caro^{1,2}, Giulia De Soricellis¹, Simone Dell'Acqua¹, Enrico Monzani^{1,*} and Stefania Nicolis^{1,*}

¹ Dipartimento di Chimica, Università di Pavia, via Taramelli 12, 27100 Pavia, Italy; silvia.decaro01@universitadipavia.it (S.D.C.); giulia.desoricellis@unipv.it (G.D.S.); simone.dellacqua@unipv.it (S.D.); enrico.monzani@unipv.it (E.M.); stefania.nicolis@unipv.it (S.N.)

² Scuola Universitaria Superiore IUSS, piazza della Vittoria 15, 27100 Pavia, Italy

* Correspondence: enrico.monzani@unipv.it (E.M.); stefania.nicolis@unipv.it (S.N.)

Supporting information

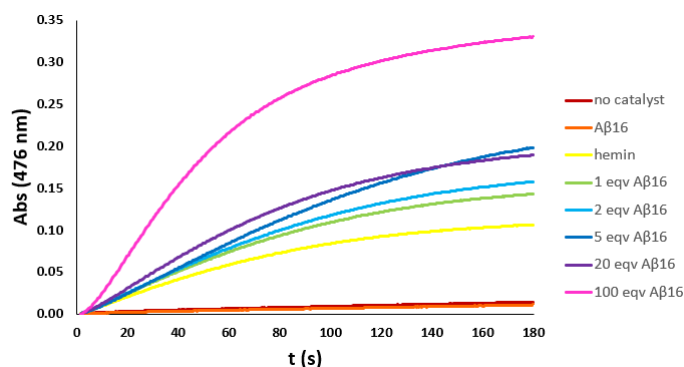


Figure S1: *kinetic trends of DA (3 mM) oxidation with H_2O_2 (50 mM) in phosphate buffer (100 mM, pH 7.4) at 25°C, with no catalyst (brown trace) and in the presence of hemin (0.2 μ M) (yellow trace), $A\beta_{16}$ (0.2 μ M) (orange trace) or hemin- $A\beta_{16}$ complex with increasing amounts of $A\beta_{16}$ (1 eqv green trace, 2 eqv light blue trace, 5 eqv blue trace, 20 eqv purple trace, 100 eqv pink trace). Both the trends with no catalyst and in presence of the peptide only are almost flat, indicating no activity.*

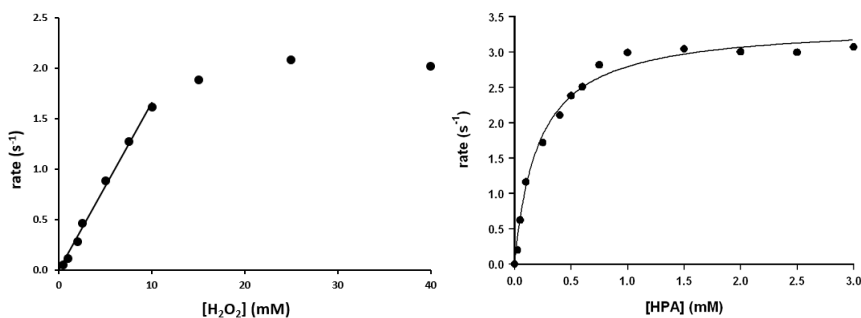


Figure S2: *trend of the initial rate of the oxidation reaction of the substrate HPA, in presence of $A\beta_{16}$ 10 μ M and hemin 2 μ M, vs $[H_2O_2]$ (left) and vs $[HPA]$ (right), in phosphate buffer 100 mM, pH 7.4 at 25°C.*

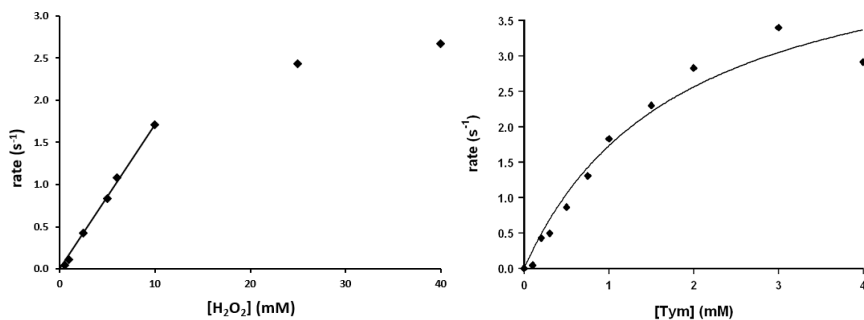


Figure S3: trend of the initial rate of the oxidation reaction of the substrate *Tym*, in presence of $A\beta_{16}$ 10 μ M and hemin 2 μ M, vs $[H_2O_2]$ (left) and vs $[Tym]$ (right), in phosphate buffer 100 mM, pH 7.4 at 25 °C.

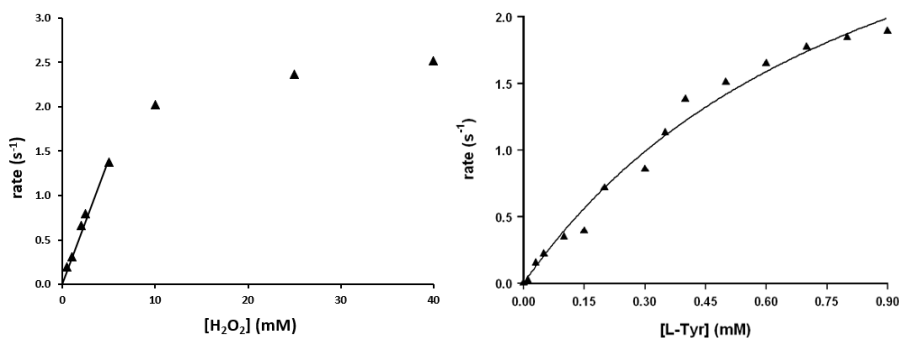


Figure S4: trend of the initial rate of the oxidation reaction of the substrate *L-Tyr*, in presence of $A\beta_{16}$ 10 μ M and hemin 2 μ M, vs $[H_2O_2]$ (left) and vs $[L-Tyr]$ (right), in phosphate buffer 100 mM, pH 7.4 at 25 °C.

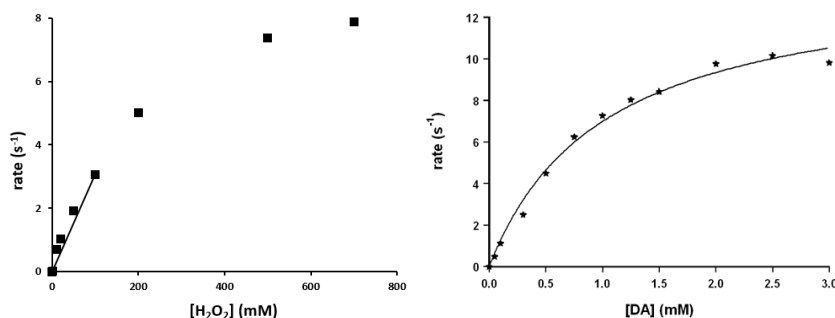


Figure S5: trend of the initial rate of the oxidation reaction of the substrate *DA*, in presence of $A\beta_{16}$ 1 μ M and hemin 0.2 μ M, vs $[H_2O_2]$ (left) and vs $[DA]$ (right), in phosphate buffer 100 mM, pH 7.4 at 25 °C.

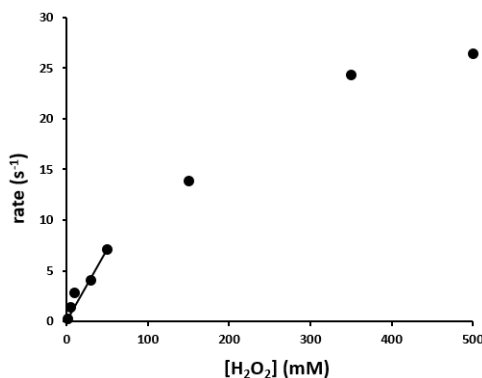


Figure S6: trend of the initial rate of the oxidation reaction of the substrate *L-DOPA*, in presence of $A\beta_{16}$ 1 μ M and hemin 0.2 μ M, vs $[H_2O_2]$, in phosphate buffer 100 mM, pH 7.4 at 25 °C.

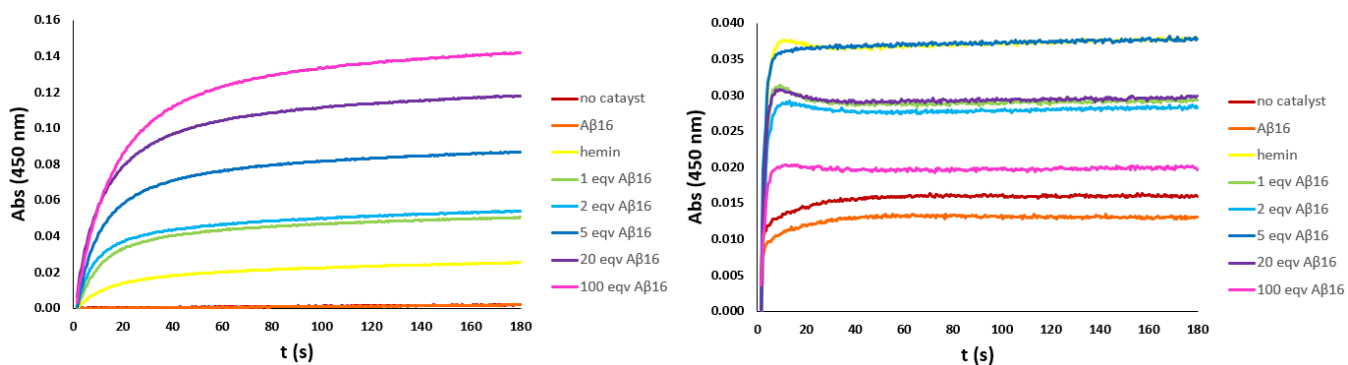


Figure S7: kinetic trends of HPA (3 mM) nitration with H_2O_2 (50 mM) and NO_2^- (500 mM) (left) and with $ONOO^-$ (0.1 mM) (right) in phosphate buffer (100 mM, pH 7.4) at 25°C, with no catalyst (brown trace) and in the presence of hemin (2 μ M) (yellow trace), $A\beta_{16}$ (2 μ M) (orange trace) or hemin- $A\beta_{16}$ complex with increasing amounts of $A\beta_{16}$ (1 eqv green trace, 2 eqv light blue trace, 5 eqv blue trace, 20 eqv purple trace, 100 eqv pink trace).

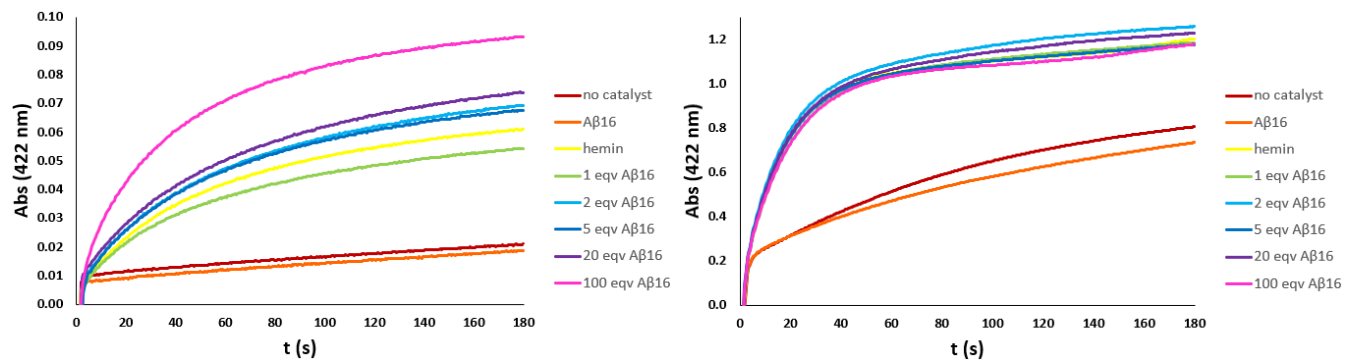


Figure S8: kinetic trends of DA (3 mM) nitration with H_2O_2 (500 mM) and NO_2^- (500 mM) (left) and with $ONOO^-$ (1 mM) (right) in phosphate buffer (100 mM, pH 7.4) at 25°C, with no catalyst (brown trace) and in the presence of hemin (0.2 μ M) (yellow trace), $A\beta_{16}$ (0.2 μ M) (orange trace) or hemin- $A\beta_{16}$ complex with increasing amounts of $A\beta_{16}$ (1 eqv green trace, 2 eqv light blue trace, 5 eqv blue trace, 20 eqv purple trace, 100 eqv pink trace).

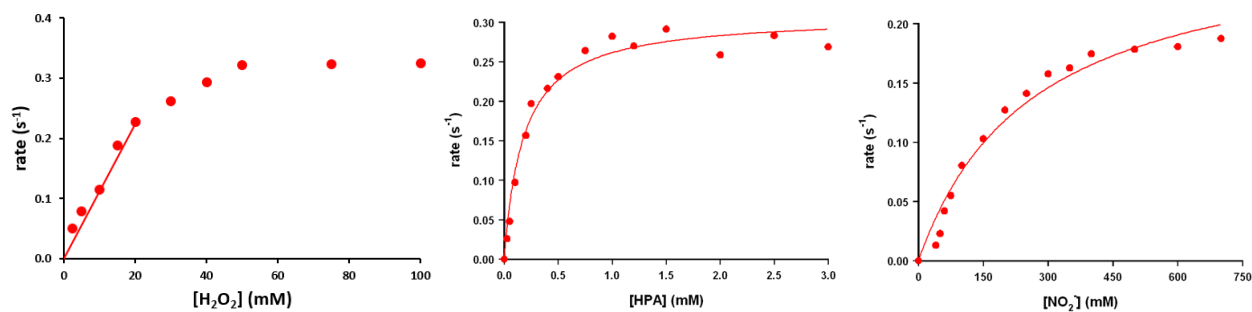


Figure S9: trend of the initial rate of the nitration reaction with H_2O_2/NO_2^- of the substrate HPA, in presence of $A\beta_{16}$ 10 μ M and hemin 2 μ M, vs $[H_2O_2]$ (left), vs $[HPA]$ (middle) and vs $[NO_2^-]$ (right), in phosphate buffer 100 mM, pH 7.4 at 25°C.

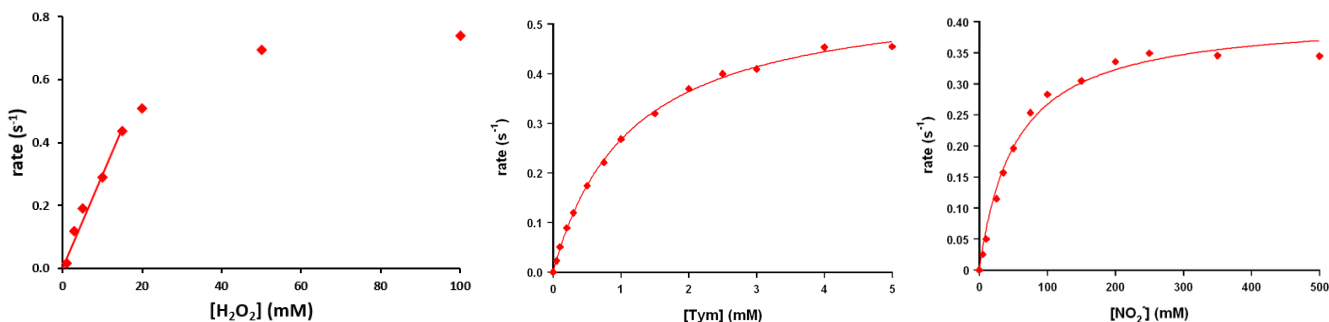


Figure S10: trend of the initial rate of the nitration reaction with H_2O_2/NO_2^- of the substrate Tym, in presence of $A\beta_{16}$ 10 μM and hemin 2 μM , vs $[H_2O_2]$ (left), vs $[Tym]$ (middle) and vs $[NO_2^-]$ (right), in phosphate buffer 100 mM, pH 7.4 at 25 $^{\circ}C$.

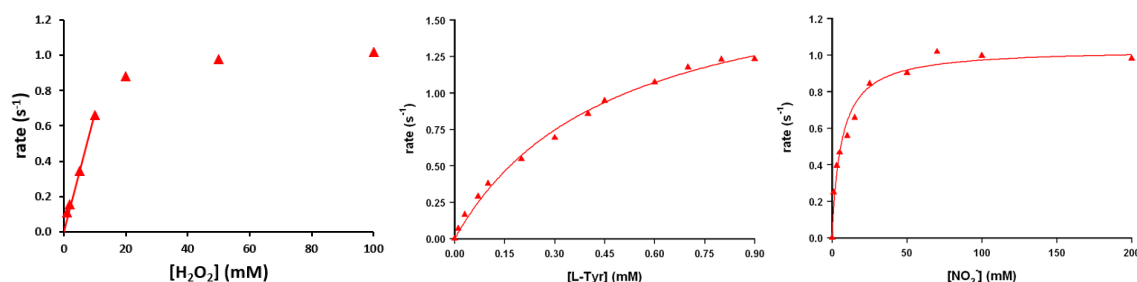


Figure S11: trend of the initial rate of the nitration reaction with H_2O_2/NO_2^- of the substrate L-Tyr, in presence of $A\beta_{16}$ 10 μM and hemin 2 μM , vs $[H_2O_2]$ (left), vs $[L-Tyr]$ (middle) and vs $[NO_2^-]$ (right), in phosphate buffer 100 mM, pH 7.4 at 25 $^{\circ}C$.

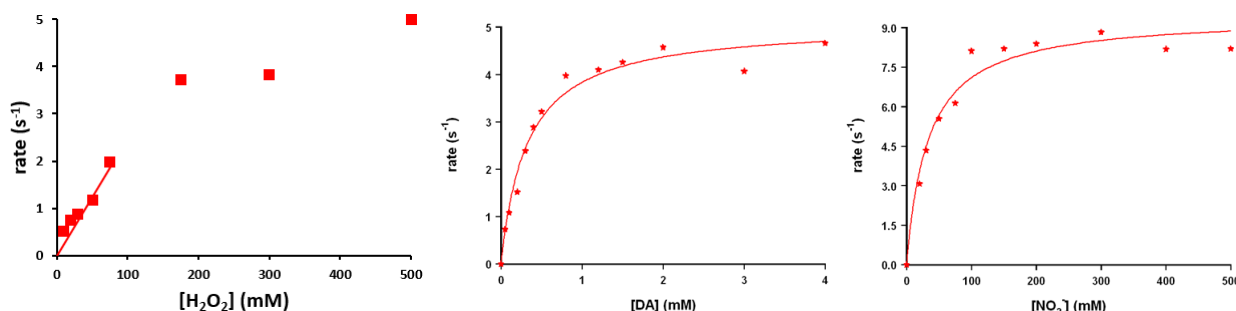


Figure S12: trend of the initial rate of the nitration reaction with H_2O_2/NO_2^- of the substrate DA, in presence of $A\beta_{16}$ 1 μM and hemin 0.2 μM , vs $[H_2O_2]$ (left), vs $[DA]$ (middle) and vs $[NO_2^-]$ (right), in phosphate buffer 100 mM, pH 7.4 at 25 $^{\circ}C$.

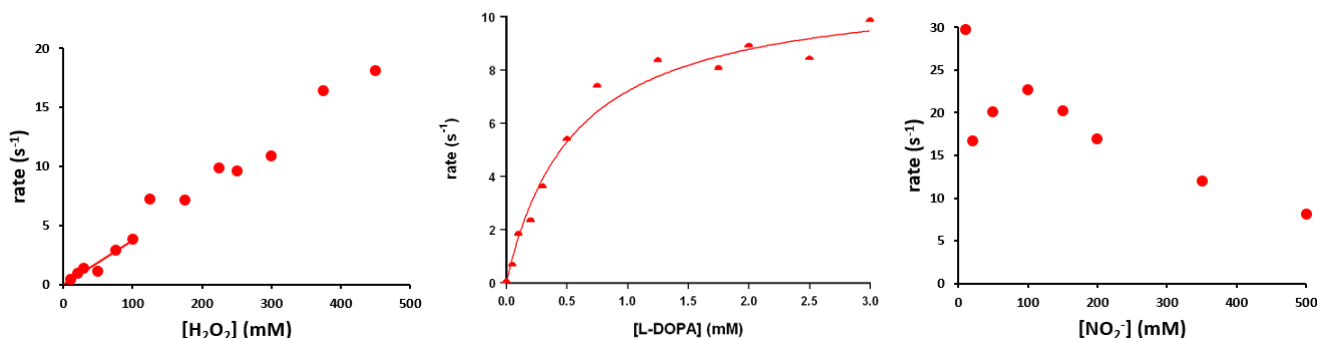


Figure S13: trend of the initial rate of the nitration reaction with H_2O_2/NO_2^- of the substrate L-DOPA, in presence of $A\beta_{16}$ 1 μM and hemin 0.2 μM , vs $[H_2O_2]$ (left), vs $[L-DOPA]$ (middle) and vs $[NO_2^-]$ (right), in phosphate buffer 100 mM, pH 7.4 at 25 $^{\circ}C$.

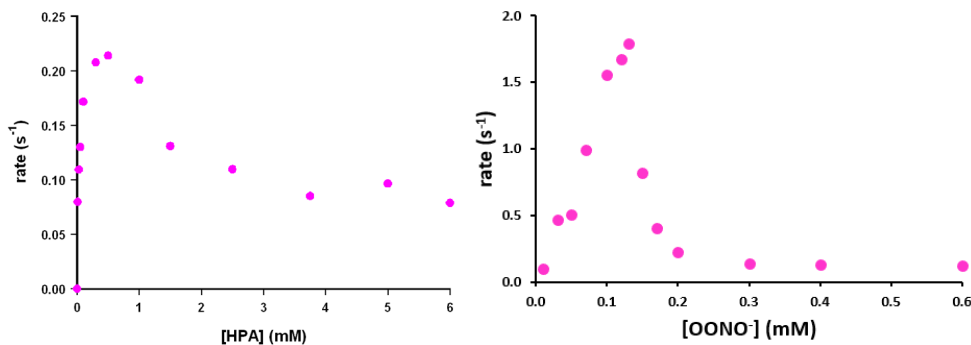


Figure S14: trend of the initial rate of the nitration reaction with $ONOO^-$ of the substrate HPA, in presence of $A\beta_{16}$ 10 μM and hemin 2 μM , vs [HPA] (left) and vs $[ONOO^-]$ (right), in phosphate buffer 100 mM, pH 7.4 at 25 °C.

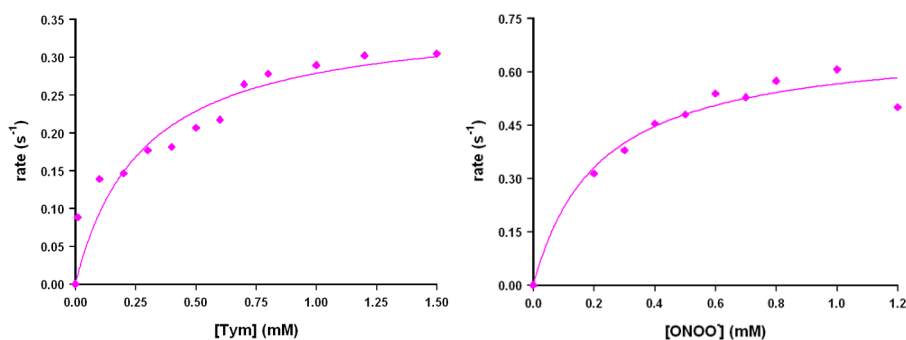


Figure S15: trend of the initial rate of the nitration reaction with $ONOO^-$ of the substrate Tym, in presence of $A\beta_{16}$ 10 μM and hemin 2 μM , vs [Tym] (left) and vs $[ONOO^-]$ (right), in phosphate buffer 100 mM, pH 7.4 at 25 °C.

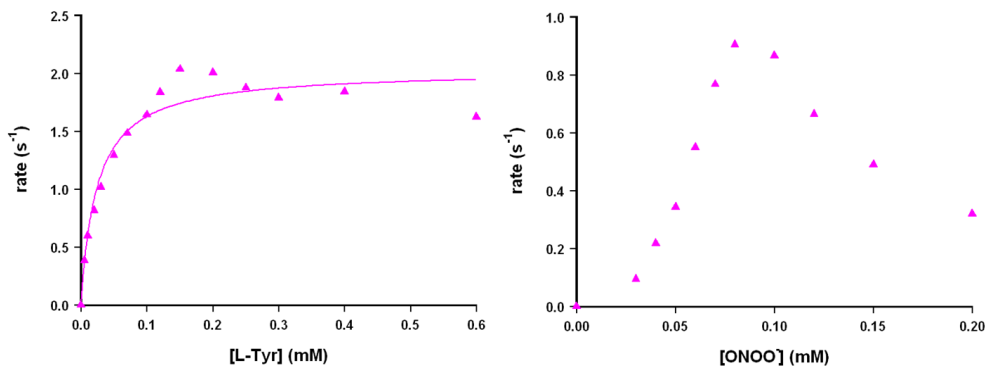


Figure S16: trend of the initial rate of the nitration reaction with $ONOO^-$ of the substrate L-Tyr, in presence of $A\beta_{16}$ 10 μM and hemin 2 μM , vs [L-Tyr] (left) and vs $[ONOO^-]$ (right), in phosphate buffer 100 mM, pH 7.4 at 25 °C.

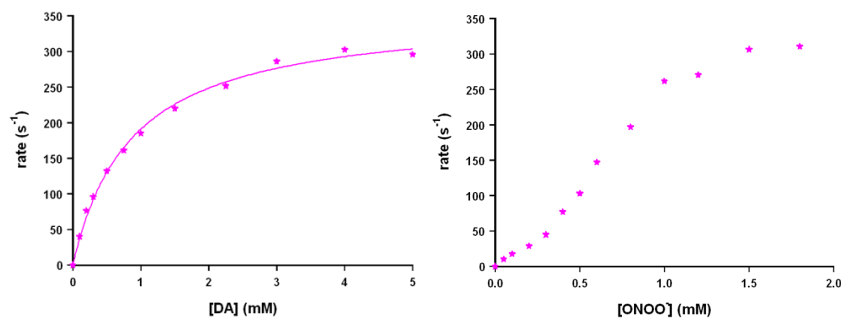


Figure S17: trend of the initial rate of the nitration reaction with $ONOO^-$ of the substrate DA, in presence of $A\beta_{16}$ 1 μM and hemin 0.2 μM , vs [DA] (left) and vs $[ONOO^-]$ (right), in phosphate buffer 100 mM, pH 7.4 at 25 °C.

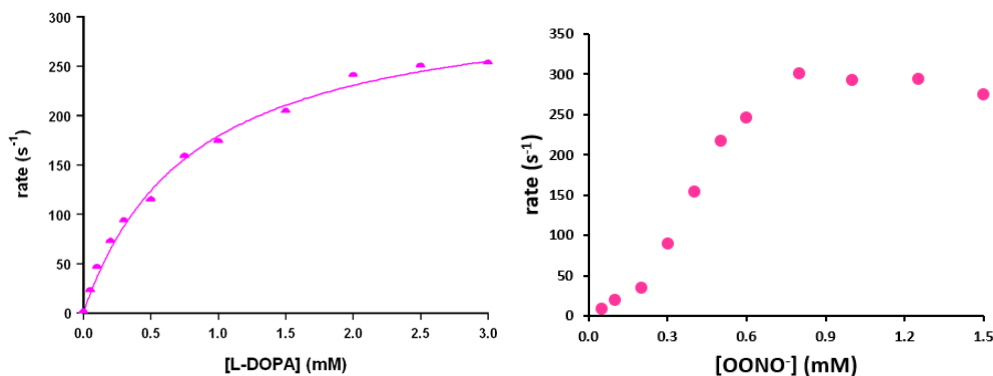


Figure S18: trend of the initial rate of the nitration reaction with ONOO^- of the substrate *L*-DOPA, in presence of $\text{A}\beta_{16}$ $1\ \mu\text{M}$ and hemin $0.2\ \mu\text{M}$, vs $[\text{L-DOPA}]$ (left) and vs $[\text{ONOO}^-]$ (right), in phosphate buffer $100\ \text{mM}$, pH 7.4 at 25°C .

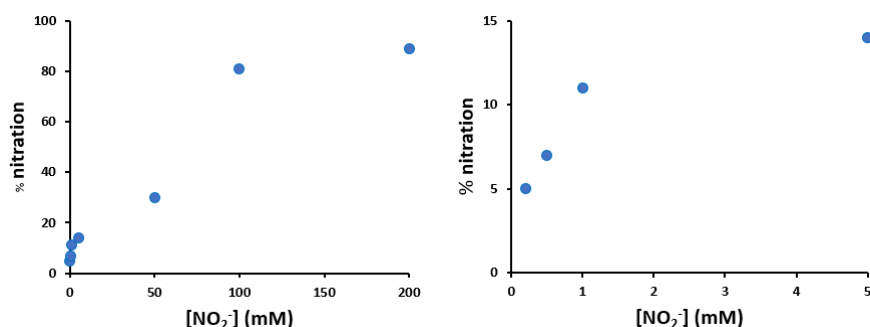


Figure S19: variation of the nitration percentage of the peptide ($10\ \mu\text{M}$), in the presence of hemin ($2\ \mu\text{M}$), as a function of the concentration of nitrite and hydrogen peroxide (both varying from 0.2 to $200\ \text{mM}$), in phosphate buffer $100\ \text{mM}$, pH 7.4 after $30\ \text{min}$ incubation at 37°C (left), and magnification of the results at low concentrations (right).

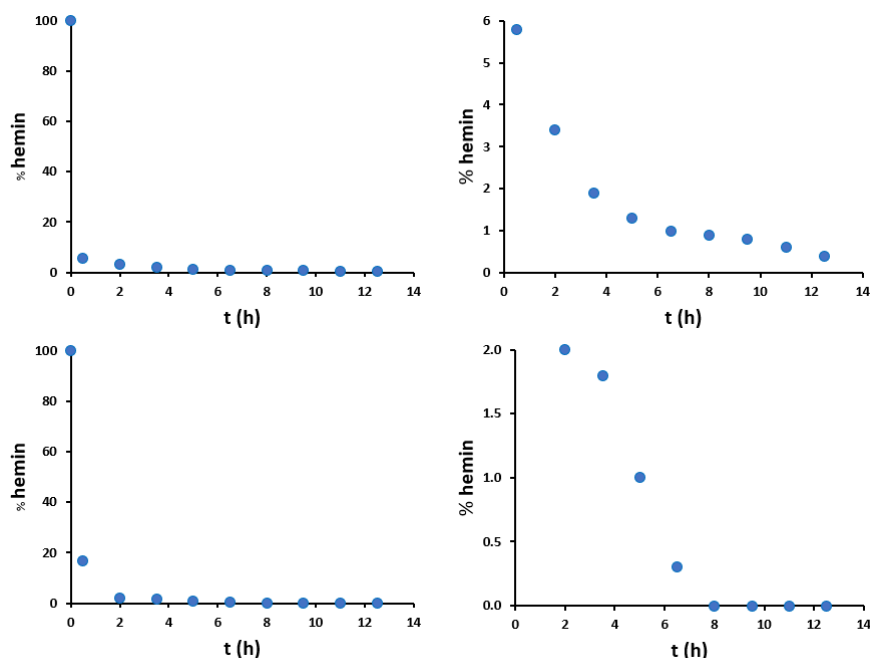


Figure S20: percentage amount of unmodified hemin as compared to the blank sample without hydrogen peroxide, in the presence of peptide ($100\ \mu\text{M}$) and hemin ($20\ \mu\text{M}$), in mild ($200\ \mu\text{M}\ \text{H}_2\text{O}_2$ / $200\ \mu\text{M}\ \text{NO}_2^-$) (up) and harsh ($20\ \text{mM}\ \text{H}_2\text{O}_2$ / $200\ \text{mM}\ \text{NO}_2^-$) (down) conditions. On the right, magnifications of the same experimental data with reduced y-axis in the range of 0 - 6% hemin and 0 - 2% hemin for mild (up) and harsh (down) conditions, respectively, are shown.